

Rapid Flow-Through Fractionation of Biomass to Preserve Labile Aryl Ether Bonds in Native Lignin

Hao Zhou,^[a] Jia Yun Xu,^[a] Yingjuan Fu,^[a] Haiguang Zhang,^[a] Zaiwu Yuan,^[a] Menghua Qin,^{*,[b]} Zhaojiang Wang^{*,[a]}

^a State Key Laboratory of Biobased Material and Green Papermaking, Qilu University of Technology, Shandong Academy of Sciences, Jinan 250353, China

^b Laboratory of Organic Chemistry, Taishan University, Taian 271021, China

Table of content

Materials	3
Gas chromatography-mass spectrometric (GC-MS) analysis and the quantification of lignin monomers.....	3
Ultra-performance liquid chromatography tandem mass spectrometry (LC-MS) analysis.....	4
Determination of structural carbohydrates and lignin in untreated biomass and solid residue after treatments.....	4
NMR analysis	5
GPC analysis	6
Schematic illustration of the Flow-through Fractionation(Figure S1)	7
HSQC spectra of the MWL of untreated wheat straw, and lignins from RFF fractionation(Figure S2)	8
Fractionated products from RFF at various treatment conditions(Figure S3).....	9
GPC Elution profile of degradation products of GG at different time(Figure S4).....	10
GC-MS identification of the low molecular weight products of GG reaction(Figure S5).....	11
LC-MS identification of the GG reaction products(Figure S6)	16
Possible mechanism of reduction reaction and oxidation reaction(Figure S7).....	19
Comparison of mass spectrum between the actually-obtained and the spectroscopy library(Figure S8).....	20
Mass spectrum of C6C3 enol-ether (EE)(Figure S9).....	27
Mass spectrum of formylated enol-ether (formylated EE)(Figure S10)	28
Yields of monomeric products from GG degradation(Figure S11)	29
Assignment of Selected ¹³ C/ ¹ H Chemical Shifts Observed in HSQC NMR Spectra(Table S1)	30

Calculation of Various Lignin Moieties by 2D NMR(Table S2)	32
Mass balances for RFF treatments of wheat straw and poplar wood(Table S3 and Table S4)	33
Peaks assignment of 2D 13C/1H HSQC NMR of GG degradation products (Table S5)	34
Literatures	35

Materials

Wheat straw was harvested from a suburb farm located at southwest of Jinan, Shandong province, China. Wheat straw was air dried and cut into lengths of 1-6 mm prior fractionation. The primary chemical compositions of the wheat straw were: cellulose 39.47%, hemicelluloses 25.31% (arabinan 2.57%, galactan 0.50%, xylan 22.24%), acid insoluble lignin 22.12%, and acid-soluble lignin 3.07%, toluene-ethanol extractives 3.21%, and ash 6.57%, according to the technical report NREL/TP-510-42623. Poplar wood logs was chipped manually to thickness of 1–5 mm. Wood chips were soak in water at room temperature for 12 hours and then grounded to fibres using a high consistency pulp-refiner (KRK 2500-II, Kumagai Riki Kogyo, Japan) with disk patterns of D2B505 and a disks-gap of 1.0 mm. The wood fibres slurry was dewatered to a solid content of about 35% by squeezing and then stored in a plastic bag at 4 °C for further use. The wood fibres were chemically composed of 38.8% cellulose, 18.2% hemicellulose (0.64% arabinan, 0.92% galactan, 14.5% xylan, and 2.24% mannan), 27.8% acid insoluble lignin, and 3.16% acid soluble lignin. Milled wood lignin (MWL) of poplar wood and wheat straw was obtained according to the classical method from extractive-free biomass.^[1] Formic acid was (ACS reagent grade), phenol, 2-methoxy-4-propyl- (PMP) and 2,4'- dihydroxy -3'-methoxyacetophenone (DMP) were purchased from Sigma-Aldrich (Saint Louis, MO, USA). Guaiacylglycerol- β -guaiacyl ether (GG), phenol, 2-methoxy- (GOH) and vanillin (VAN) were purchased from Aladdin Bio-Chem Technology (Shanghai, China). All of the other chemicals were of analytical grade and used as supplied.

Gas chromatography-mass spectrometric (GC-MS) analysis and the quantification of lignin monomers

GC-MS analysis was performed on an Agilent Technologies 7890A gas chromatograph equipped with a 5975C inert MSD/DS Turbo Electron Impact mass spectrometer employing a HP-5MS column (30 m x 0.25 mm x film thickness 0.25 μ m, Agilent Technologies). Temperature program as follows: 50°C for 3 min; ramp to 100°C at 5°C/min and hold for 5min; ramp to 280°C at 50°C /min and hold for 4 min, total run time:

25.6 min. Standard compounds from commercial purchase were used to make calibration curves for the quantification of GG, GOH, VAN, PMP and DMP by GC-MS. BDME and PHHM were not commercially available, and quantified by using the calibration curve of VAN.

Ultra-performance liquid chromatography tandem mass spectrometry (LC-MS) analysis

LC-MS quantitation of depolymerization products was performed via gradient elution from an Ascentis Express C18 column (150 mm x 2.1 mm x 2.7 μm particle size, Supelco, Bellefonte, PA) followed by integration of extracted ion chromatograms of [M-H]⁻ ions. A quadrupole-Orbitrap hybrid mass spectrometer (Q Exactive, Thermo Scientific, San Jose, CA) equipped with a heated electrospray source (HESI II Probe, Thermo Scientific) and a photodiode array UV detector (Accela PDA Detector, Thermo Scientific) were used to detect analytes. The system was fitted with an autosampler that kept samples at 4 °C prior to injection (Thermo PAL, Thermo Scientific). Mobile phase A consisted of water with 0.1% formic acid adjusted to pH 3 with ammonia and B was acetonitrile. The gradient program at 0.4 mL/min flow rate and ambient temperature was: 10% B for 1 min, to 20% B over 14 min, to 70% B over 5 min, and held there for 5 min before immediately returning to initial conditions and re-equilibrating for 4 min. The mass spectrometer was operated in fast polarity switching mode, acquiring full scan (85 – 500 Th, R = 17,500, AGC Target = 5e5, max. injection times = 50 ms (+), 75 ms (-), centroid acquisition, S-lens = 50, and inlet = 320 °C) mass spectra in positive and negative ion mode during the same chromatographic run. The source conditions were as follows: Source heater at 350 °C and 60 and 15 units each of sheath and auxiliary gas. The UV detector acquired spectra (190–500 nm) at 5 Hz in addition to absorbance traces at 254, 280, and 322 nm. Filter bandwidth and wavelength step were 1 nm each for acquisition of spectra and filter bandwidth was 9 nm for single wavelength UV trace acquisition. Filter rise time was set to 0.2 s.

Determination of structural carbohydrates and lignin in untreated biomass and solid residue after treatments

The structural carbohydrates and lignin in untreated biomass and the solid residue after treatment were determined according to technical

report NREL/TP-510-42618.^[2] Saccharides and degradation products in liquid extract were determined according to technical report NREL/TP-510-42623.^[3] Monosaccharides were determined directly using a Dionex HPLC system (ICS-5000, Sunnyvale, CA) equipped with a GP40 gradient pump, an anion exchange column (CarboPac PA20 analytical column 3×150 mm and guard column 3×30 mm) and an ED40 electrochemical detector as described previously.^[4] To determine the amount of oligosaccharides extracted, a posthydrolysis process of the extracted liquor was performed to break all the oligomers in monomers using 4% w/w of H₂SO₄ at 120 °C for 60 min. The total lignin content in biomass was determined as a sum of acid insoluble lignin and acid-soluble lignin. The equation $1 - L_{sr} \times Y_{sr} / L_{ub}$ was used for delignification value (lignin yield), where L_{sr} is lignin content in solid residue, Y_{sr} is yield of solid residue after treatment, and L_{ub} is lignin content in untreated biomass.

NMR analysis

Dissolved lignin in extract was isolated as precipitates by 4 times dilution of extract using water, and then lyophilized at -55 °C for NMR analysis. 2D HSQC NMR of lignin was performed in a Bruker AVIII 400 MHz spectrometer according to published methods.^[5] For 2D HSQC, lignin (60 mg) was placed into a 5 mm NMR tube and dissolved in 0.5 mL of DMSO-d₆, referenced at 39.5/2.5 ppm. The 13C-1H short range correlation experiment was performed using the Bruker standard pulse program hsqcedetgpsisp2.2 (phase sensitive, gradient-edited, sensitivity enhanced 2D-HSQC using adiabatic pulses for inversion and refocusing) using non-uniform sampling of 50%. Spectra were acquired using 40 scans and an interscan delay of 1s for a total acquisition time of 3 hours with a 12 ppm sweep width in F2 (1H) using 1024 data points for an acquisition time of 85 ms; and in F1 (13C), a 215 ppm sweep width using 512 increments for acquisition time of 9.74 ms. Data processing used squared cosine-bell in F1 and F2 resulting in a 1024 × 1024 data matrix. Topspin 3.7p17 was used for interactive integration of 2D cross-peaks.

GPC analysis

The degradation products of GG at different time were estimated on a Waters Alliance Separations Module e2695 system equipped with three tandem 300 mm × 7.8 mm (L. × I.D.) Phenogel 5U columns (10000, 500, and 50 Å, respectively) and a 50 mm × 7.8 mm (L. × I.D.) Phenogel 5U guard column (Phenomenex, Torrance, CA). The eluent was an isocratic 100% THF (HPLC grade without a stabilizer) at a flow rate of 1.0 ml/min and the column temperature was maintained at 30 °C. Each sample in THF was injected after passing through a 0.45 µm filter and the fractionated lignin in the column eluent was detected using a variable wavelength detector (VWD) at 280 nm. The apparent molecular weight was calibrated using polystyrene standards and GG at 254 nm.

Schematic illustration of the Flow-through Fractionation(Figure S1)

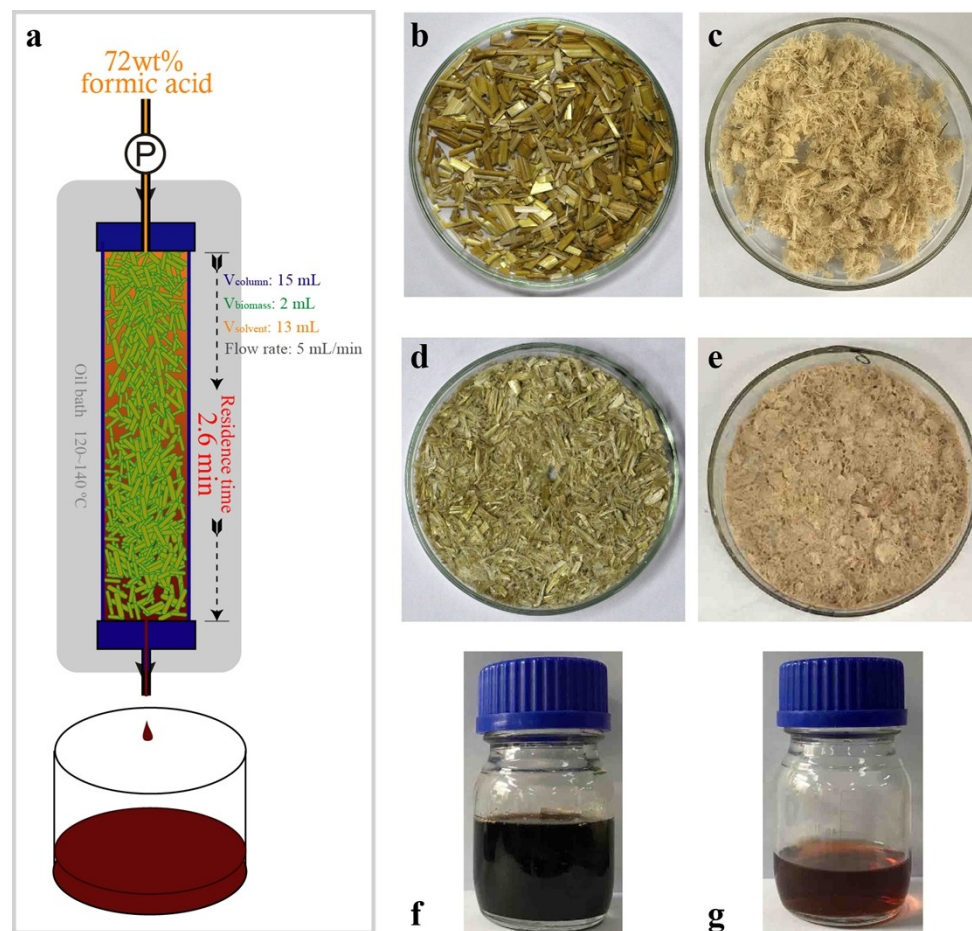


Figure S1. Rapid flow-through fractionation (RFF) of biomass using 72% aqueous formic acid. (a) configuration of flow-through reactor, untreated wheat straw and poplar wood fibers (b,c), cellulose-rich solid residue (d, e) and extract (f, g) from RFF treatment of wheat straw and poplar wood

HSQC spectra of the MWL of untreated wheat straw, and lignins from RFF fractionation(Figure S2)

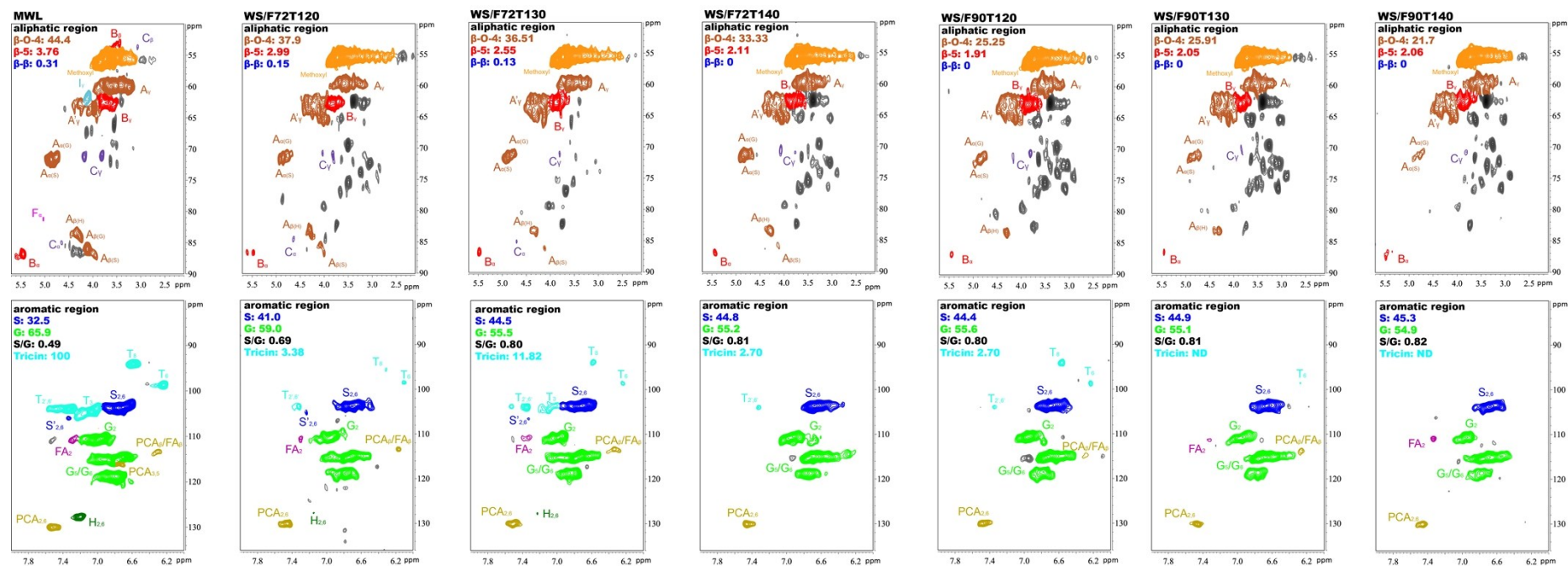


Figure S2. HSQC Spectra of the MWL of untreated wheat straw, and lignins from RFF fractionation

Fractionated products from RFF at various treatment conditions(Figure S3)

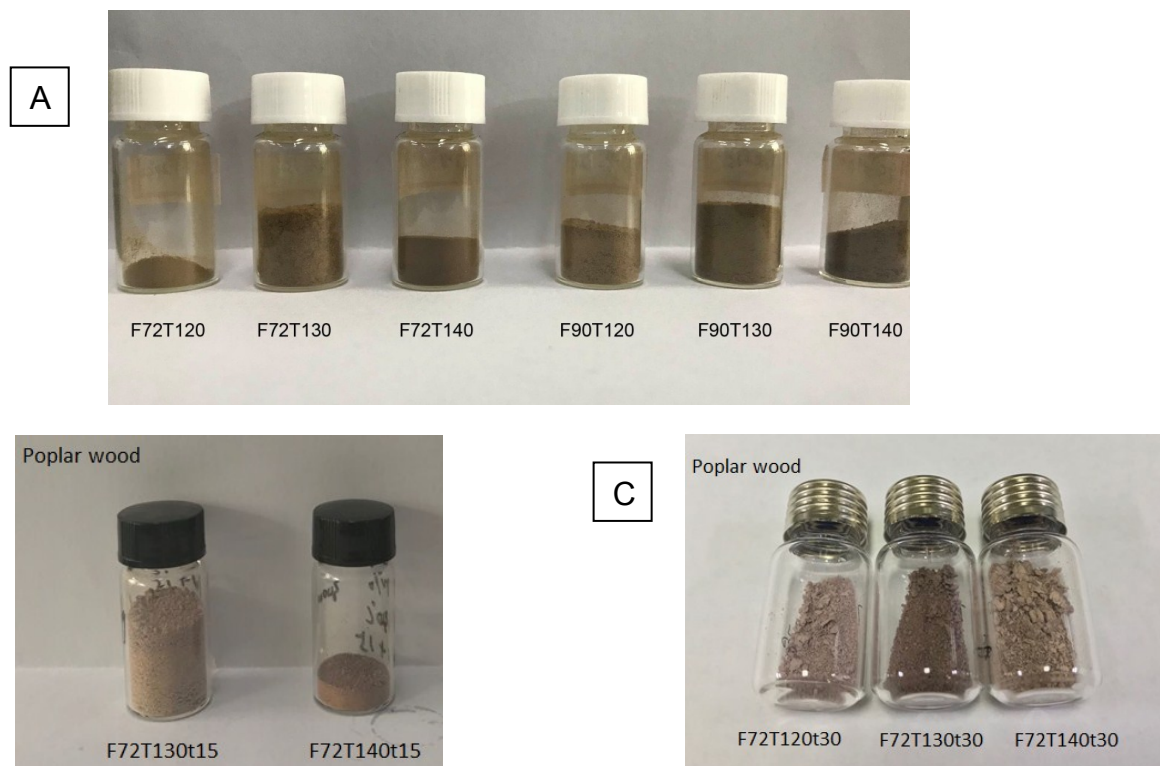


Figure S3. Fractionated products from RFF at various treatment conditions. (A) Water precipitated lignins from wheat straw effluents;(B,C) Water precipitated lignins from poplar wood effluents with different time.

GPC Elution profile of degradation products of GG at different time(Figure S4)

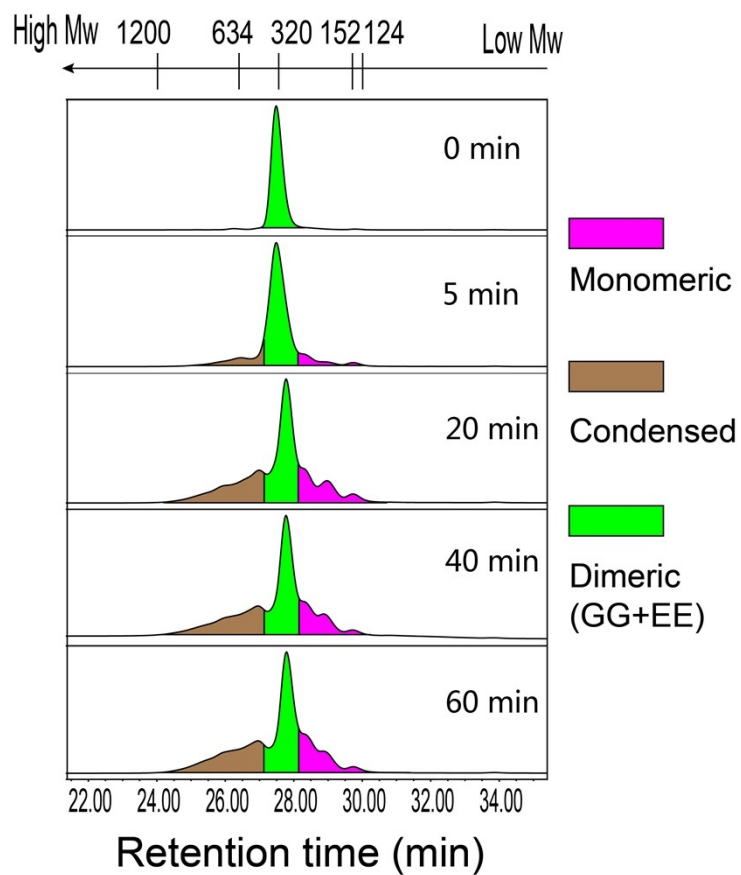
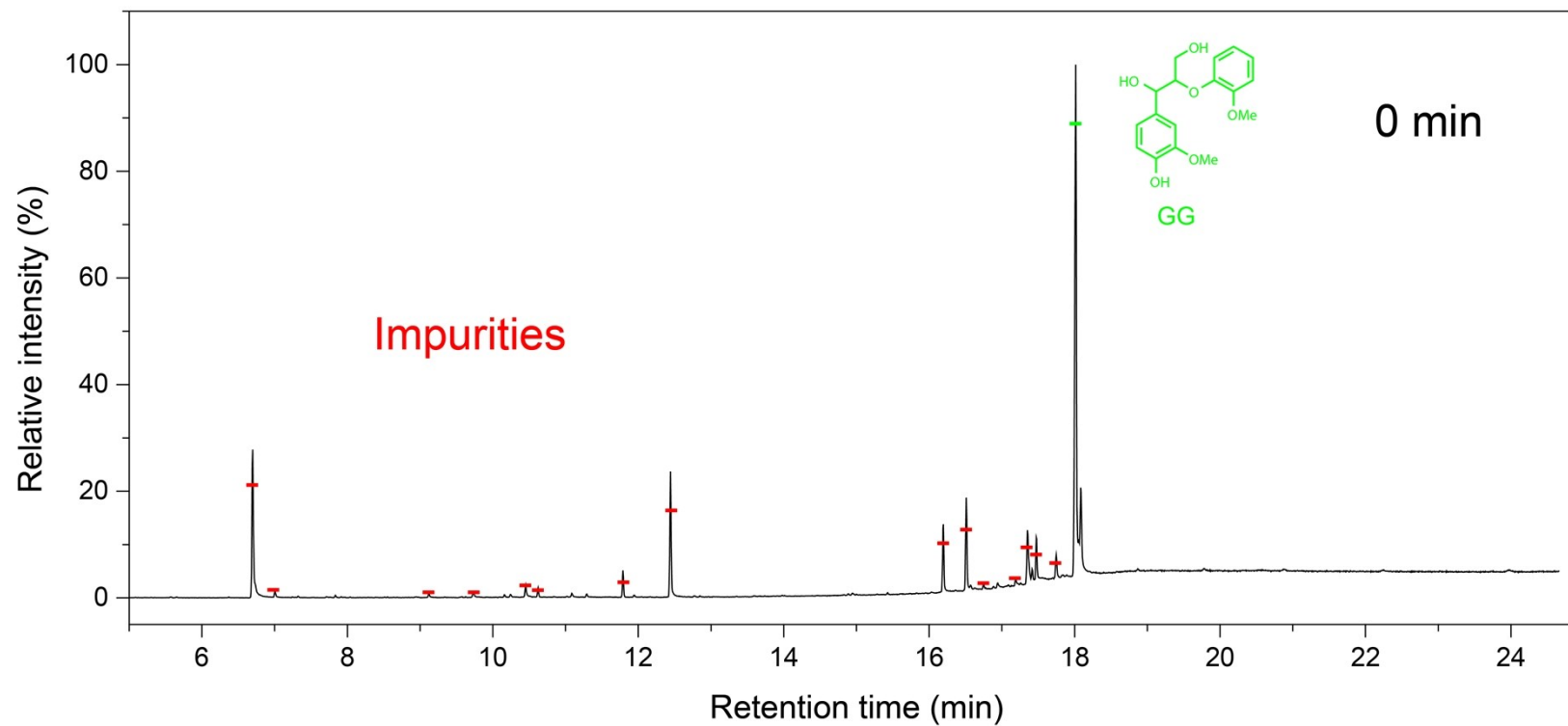
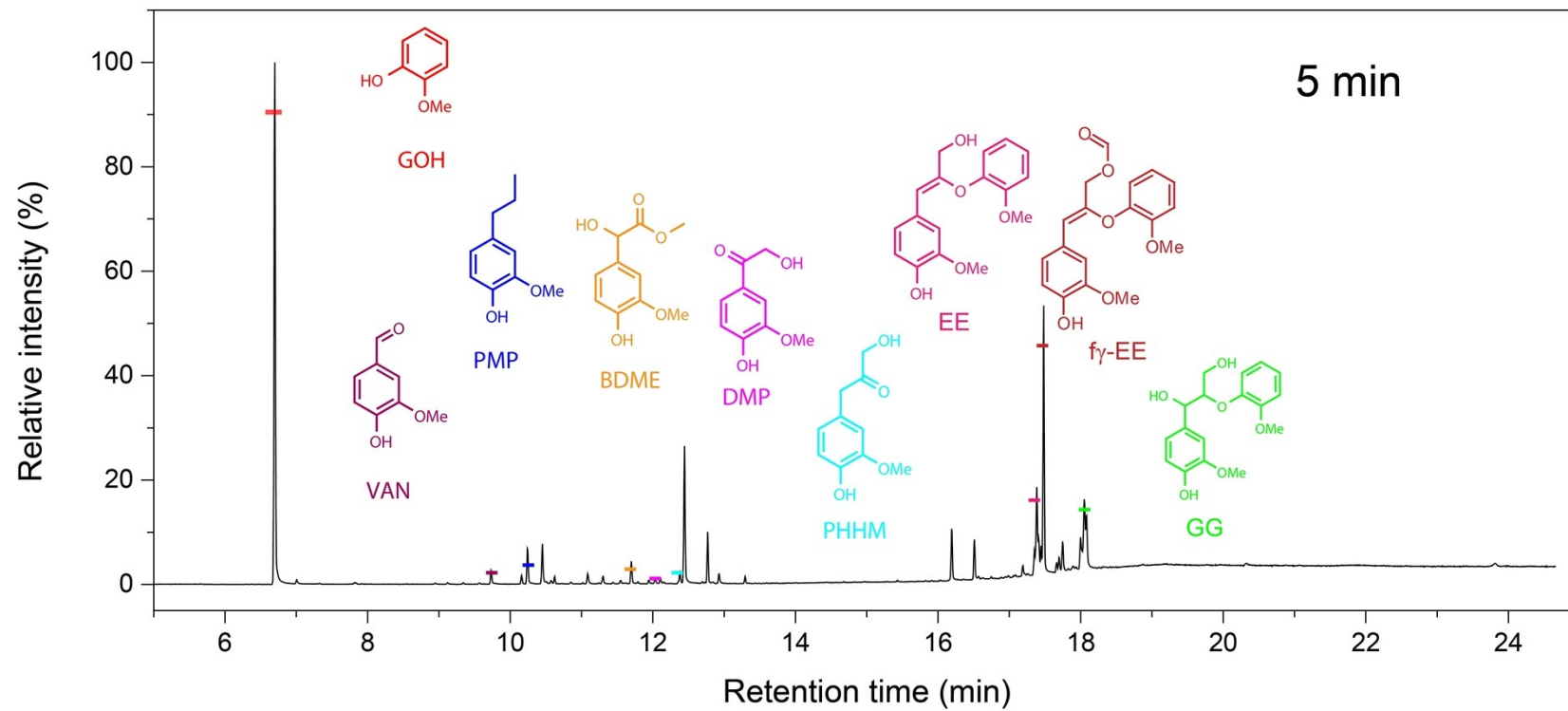
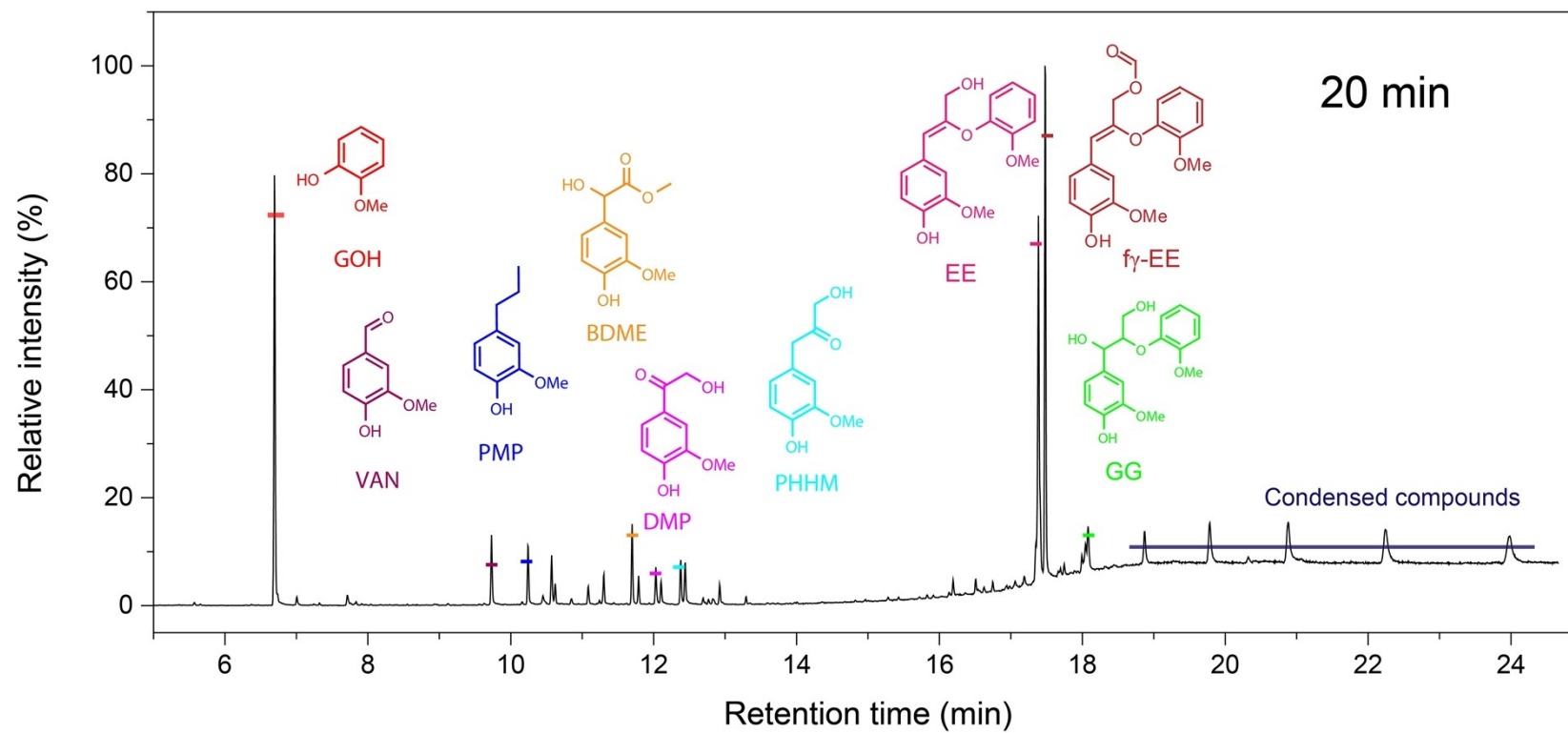


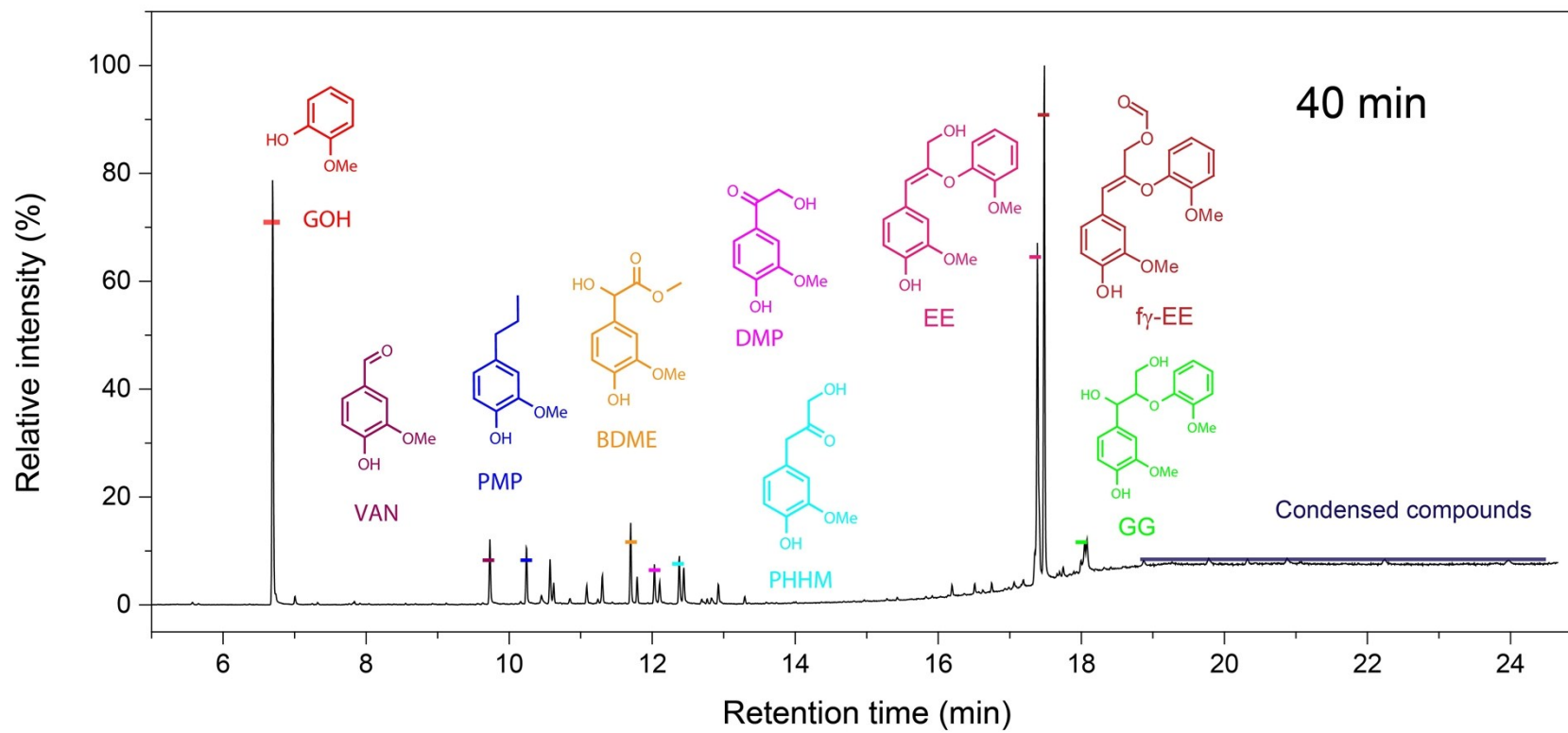
Figure S4. GPC Elution profile of degradation products of GG at different time

GC-MS identification of the low molecular weight products of GG reaction(Figure S5)









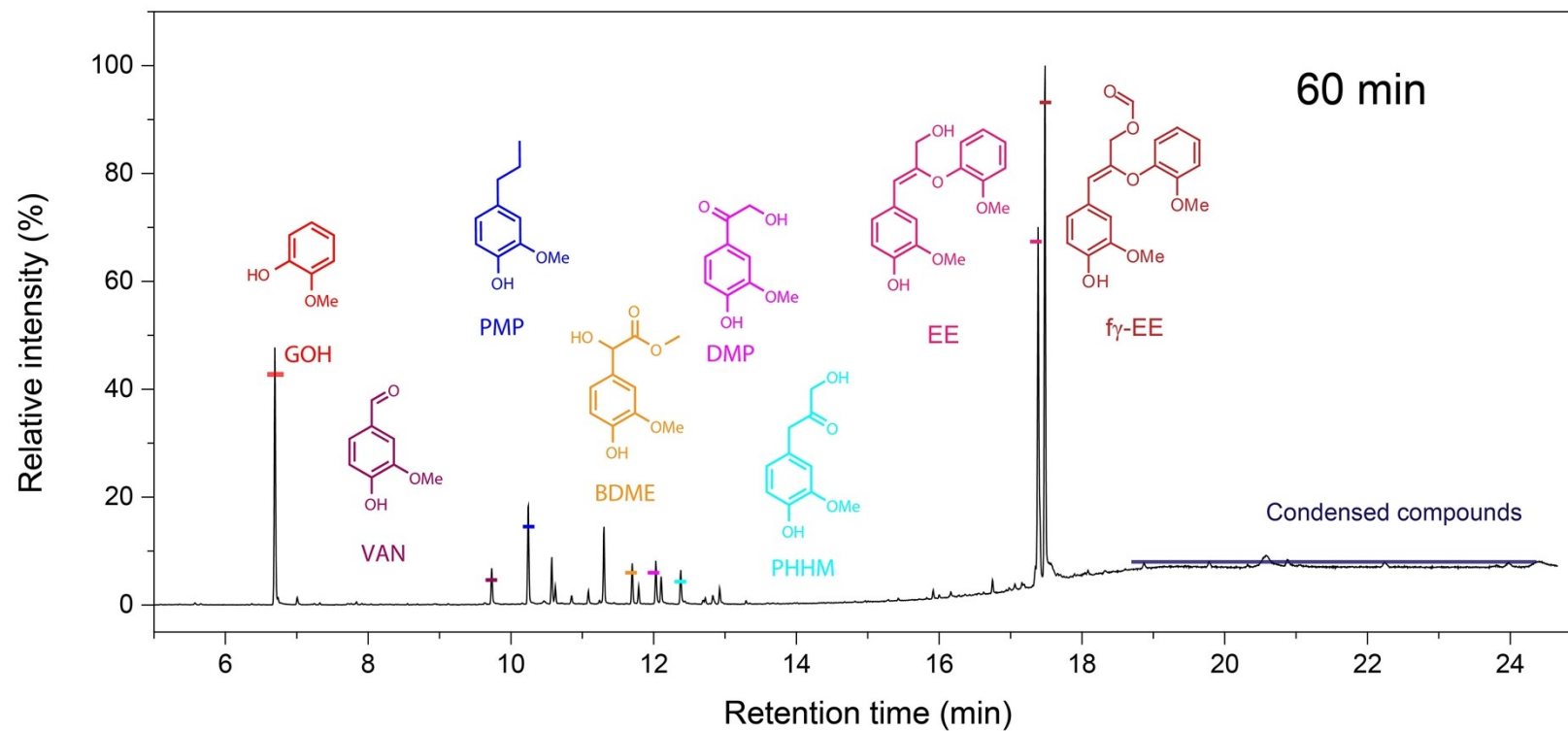
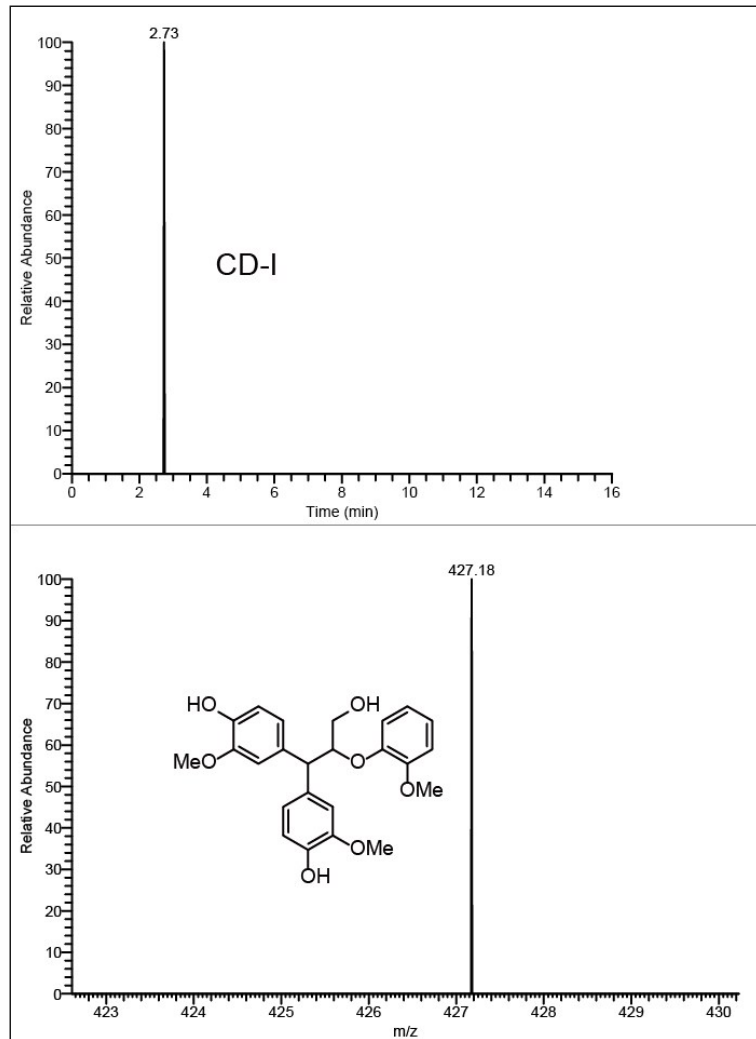


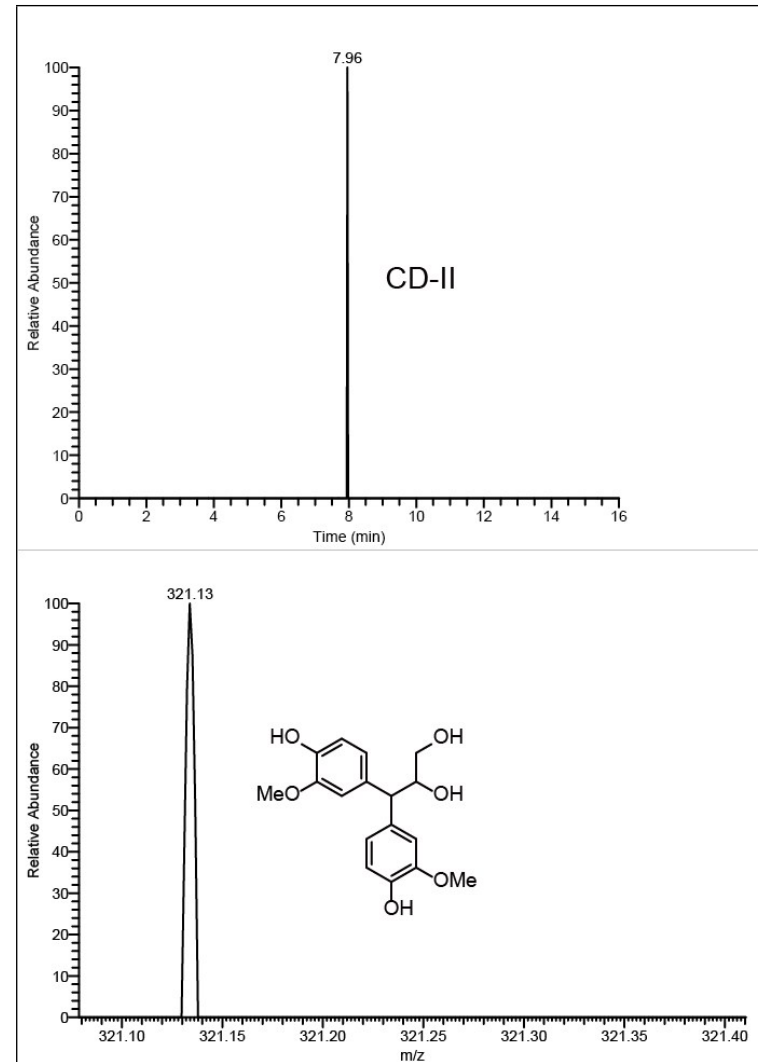
Figure S5. GC-MS identification of the low molecular weight products of GG reaction

LC-MS identification of the GG reaction products(Figure S6)

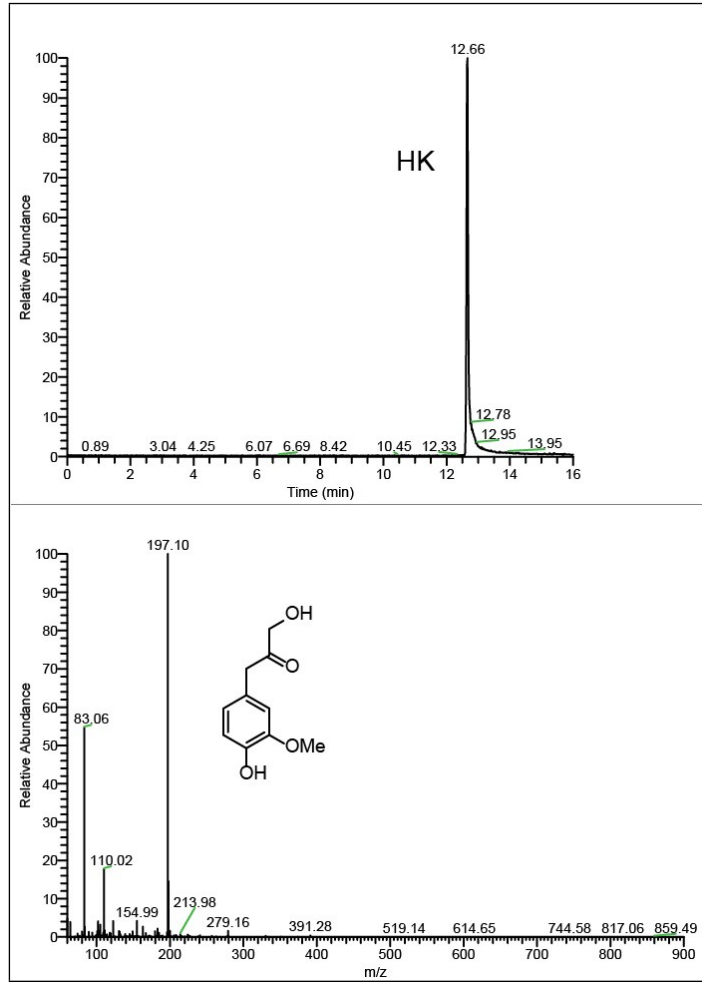
A



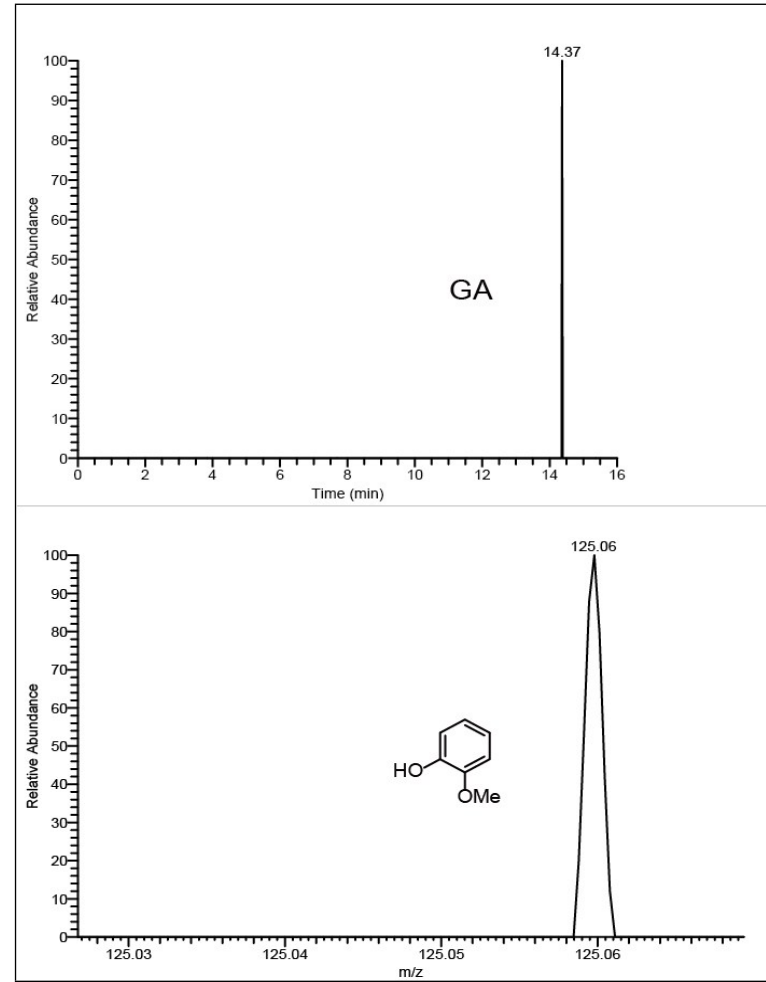
B



C



D



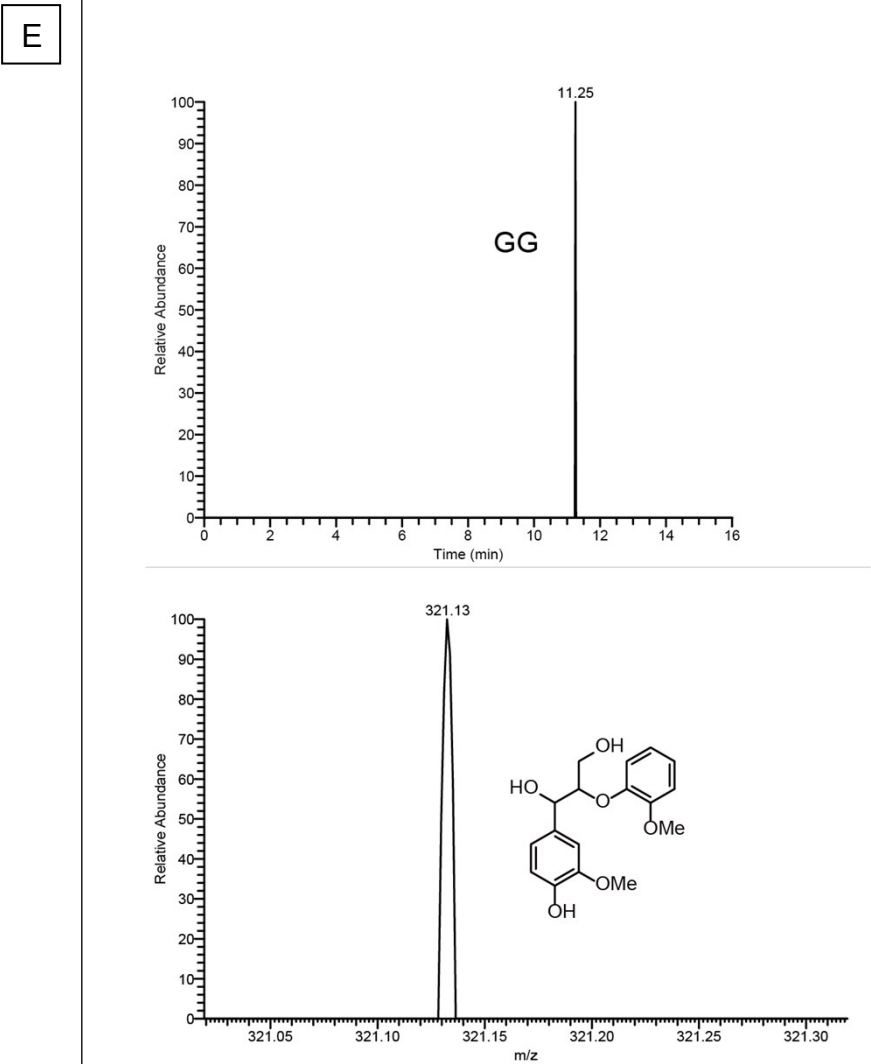
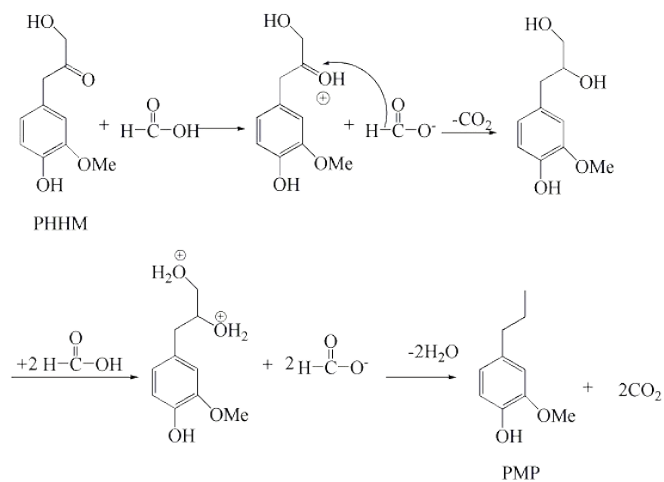


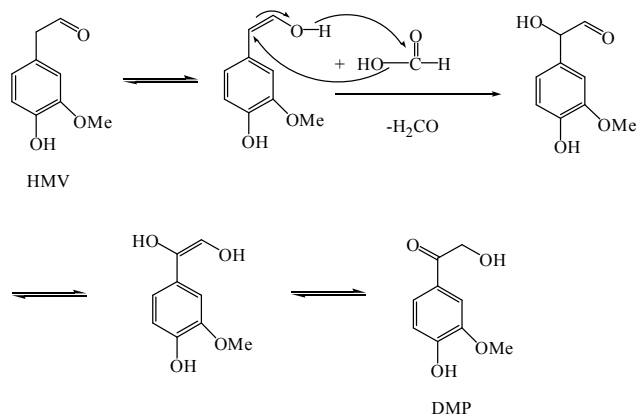
Figure S6. LC-MS identification of the GG reaction products at 130 °C with 72wt % aqueous formic acid for 20 min (A, B, C, D) and untreated GG (E).

Possible mechanism of reduction reaction and oxidation reaction(Figure S7)

(a)



(b)



(c)

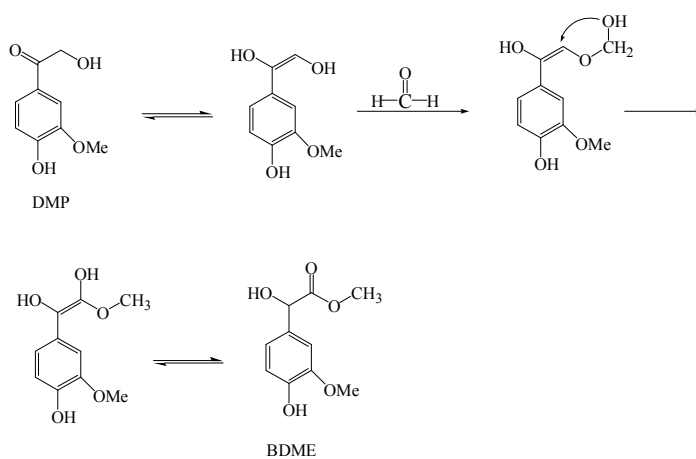
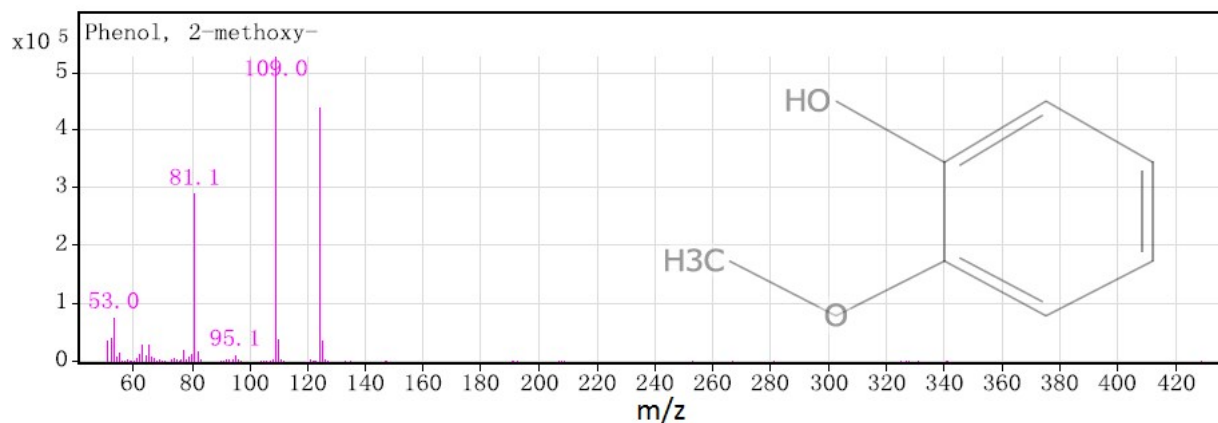
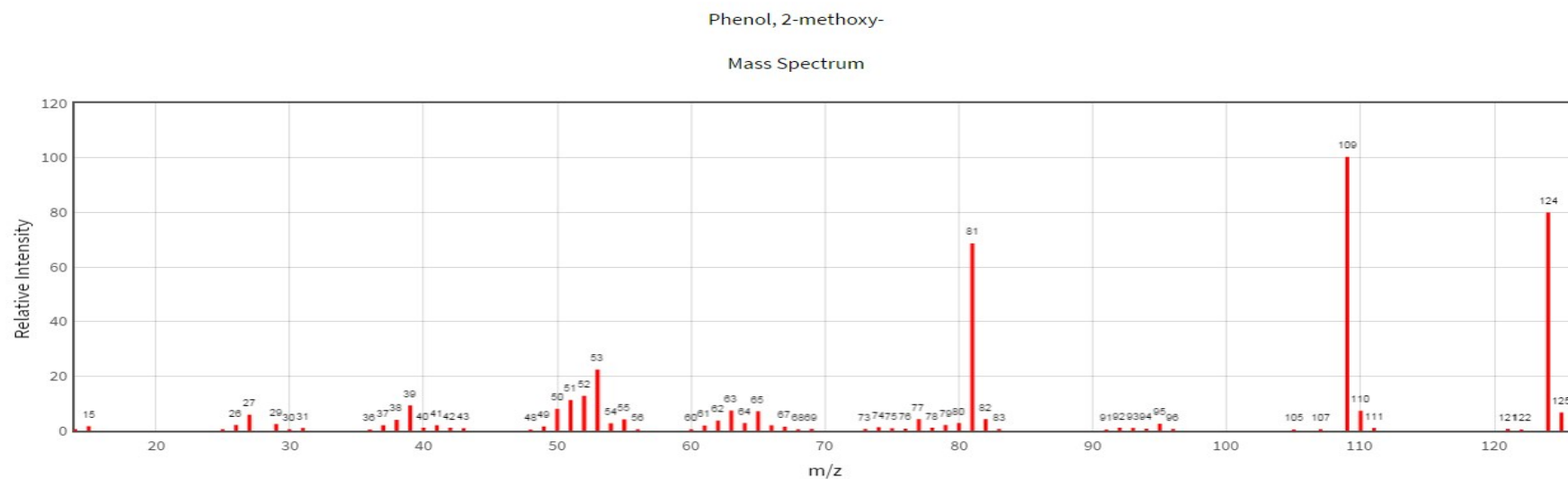


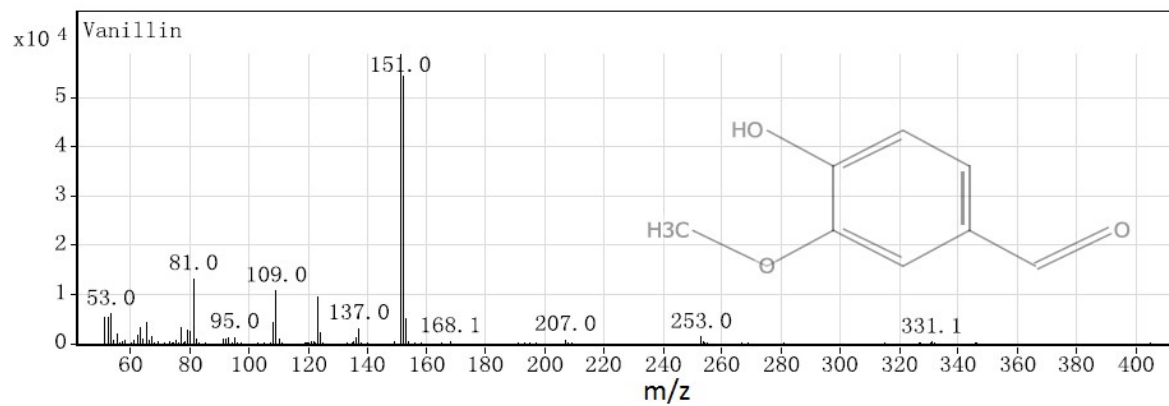
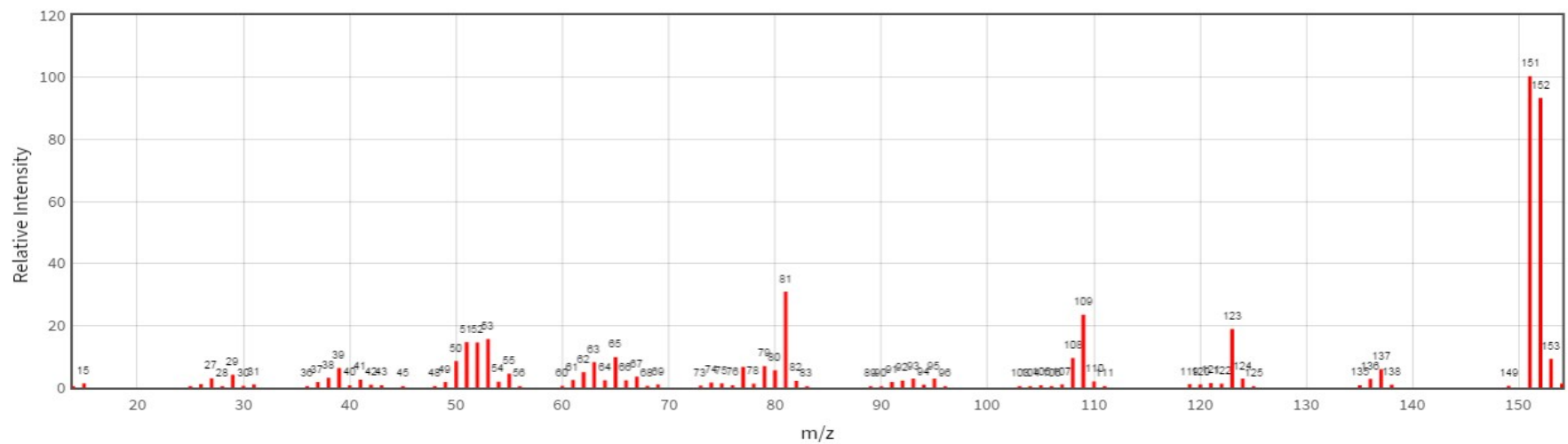
Figure S7. Possible mechanism of (a) reduction reaction of PPHM to PMP, (b) oxidation reaction of HMV to DMP, and (c) oxidation reaction of DMP to BDMP via treatment with formic acid

Comparison of mass spectrum between the actually-obtained and the spectroscopy library(Figure S8)



The mass spectrum of Phenol, 2-methoxy- (GOH) from NIST library (Top) and GC-MS (Bottom)
Compound CID: 460
CAS Registry Number: 90-05-1

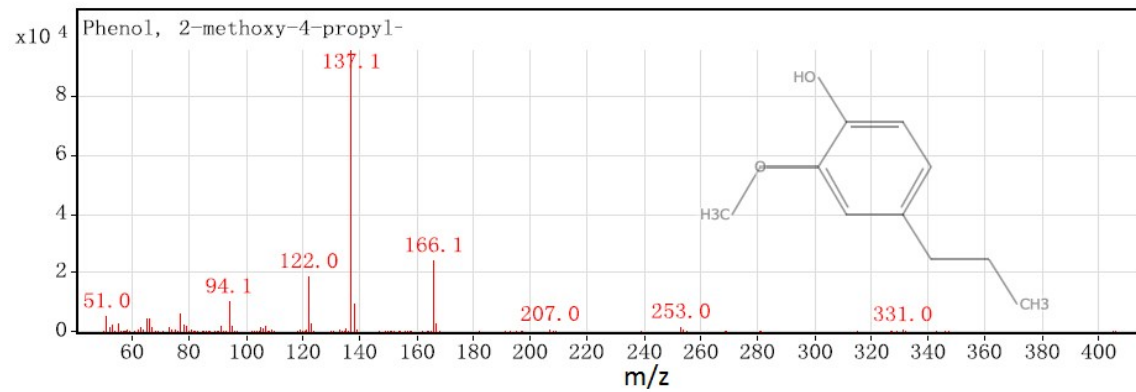
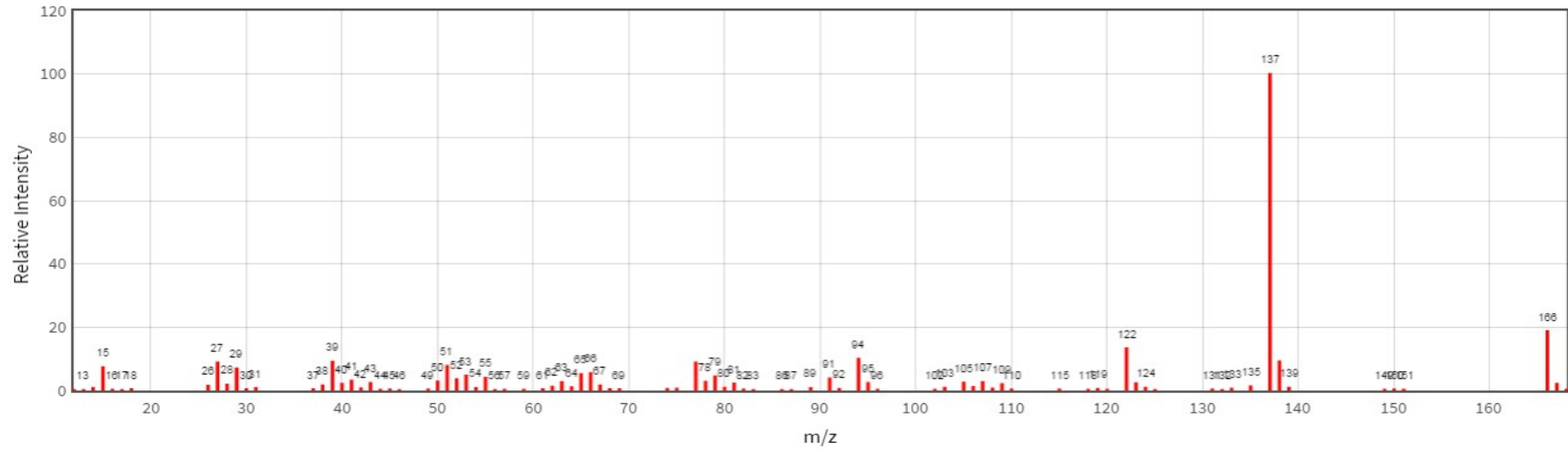
Vanillin
Mass Spectrum



The mass spectrum of Vanillin
(VAN) from NIST library (Top) and
GC-MS (Bottom)
Compound CID: 1183
CAS Registry Number: 121-33-5

Phenol, 2-methoxy-4-propyl-

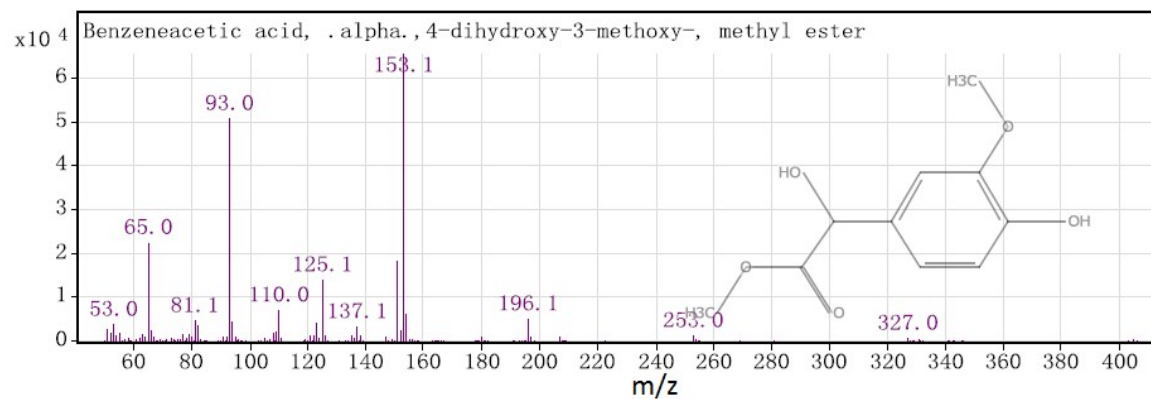
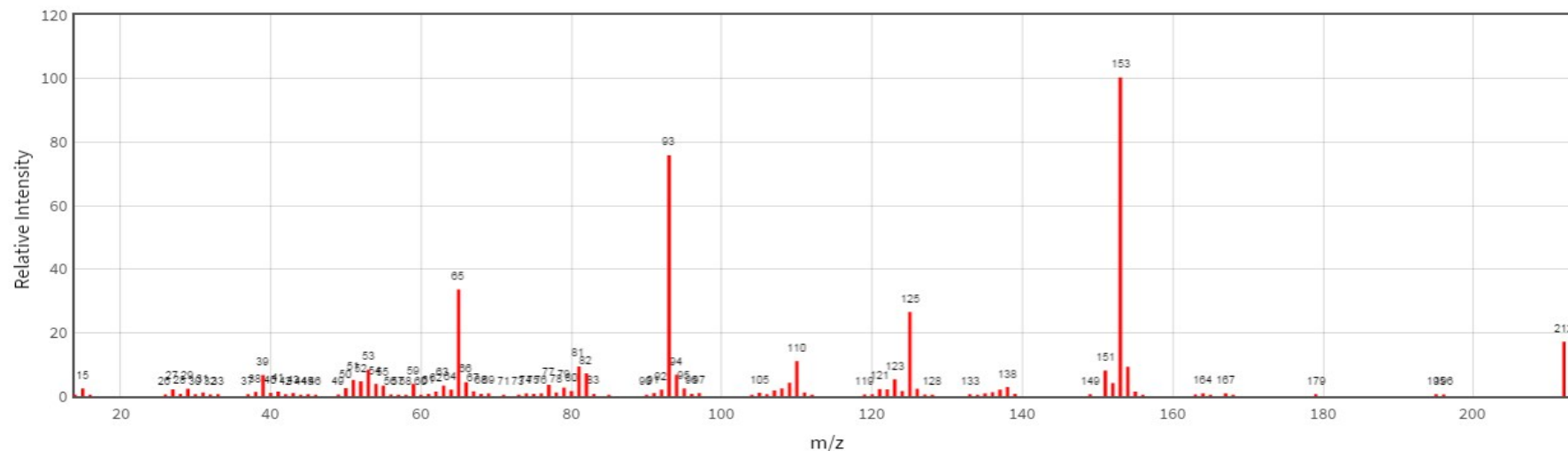
Mass Spectrum



The mass spectrum of Phenol, 2-methoxy-4-propyl- (**PMP**) from NIST library (Top) and GC-MS (Bottom)
Compound CID: 17739
CAS Registry Number: 2785-87-7

Benzeneacetic acid, .alpha.,4-dihydroxy-3-methoxy-, methyl ester

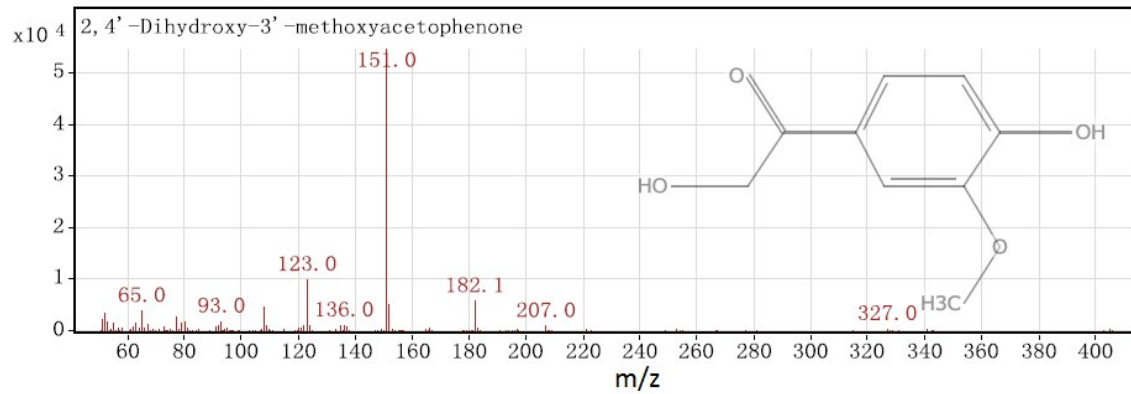
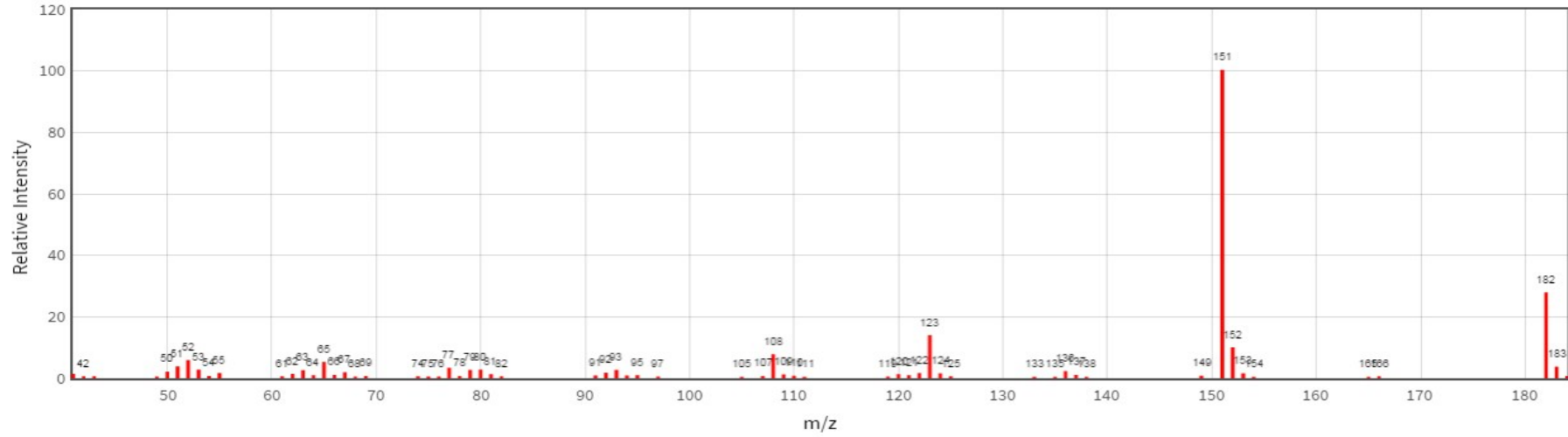
Mass Spectrum



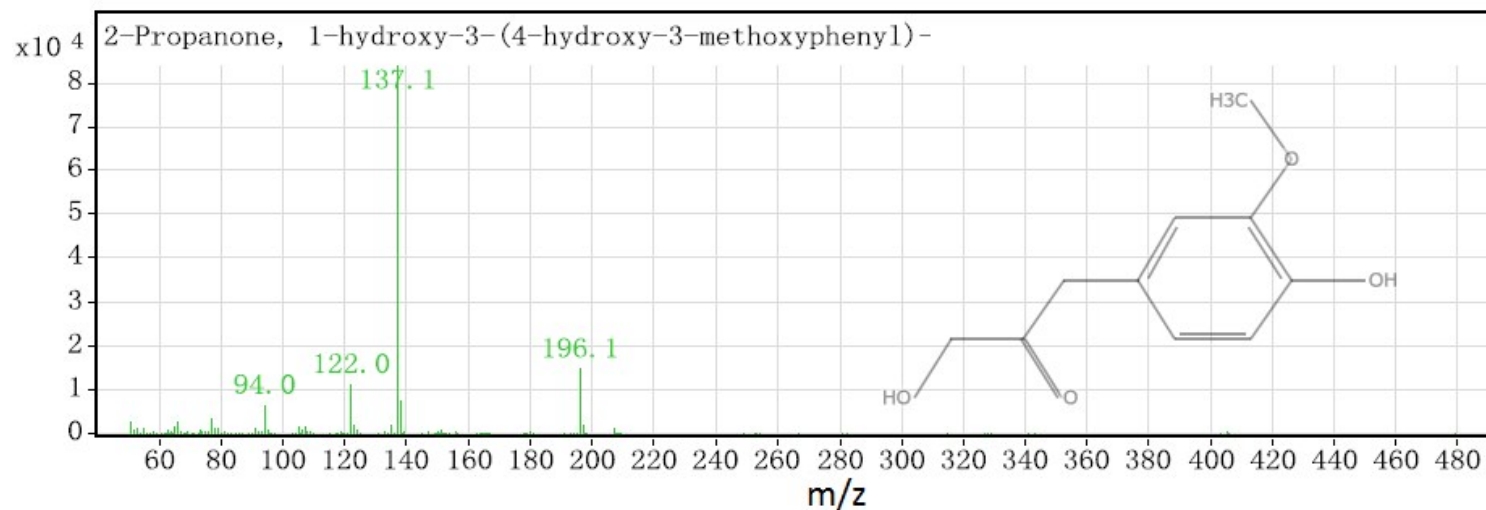
The mass spectrum of Benzeneacetic acid, .alpha.,4-dihydroxy-3-methoxy-, methyl ester (**BDME**) from NIST library (Top) and GC-MS (Bottom)
Compound CID: 592691
CAS Registry Number: 2911-74-2

2,4'-Dihydroxy-3'-methoxyacetophenone

Mass Spectrum

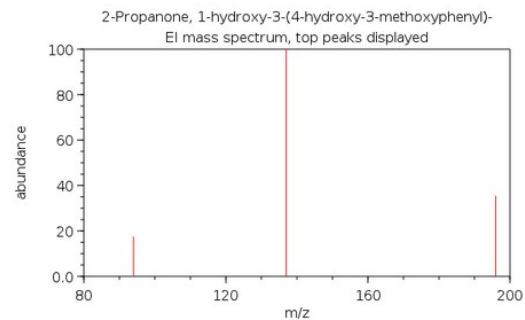


The mass spectrum of 2,4'- Dihydroxy -
3'-methoxyacetophenone (**DMP**) from
NIST library (Top) and GC-MS (Bottom)
Compound CID: 87530
CAS Registry Number: 18256-48-9

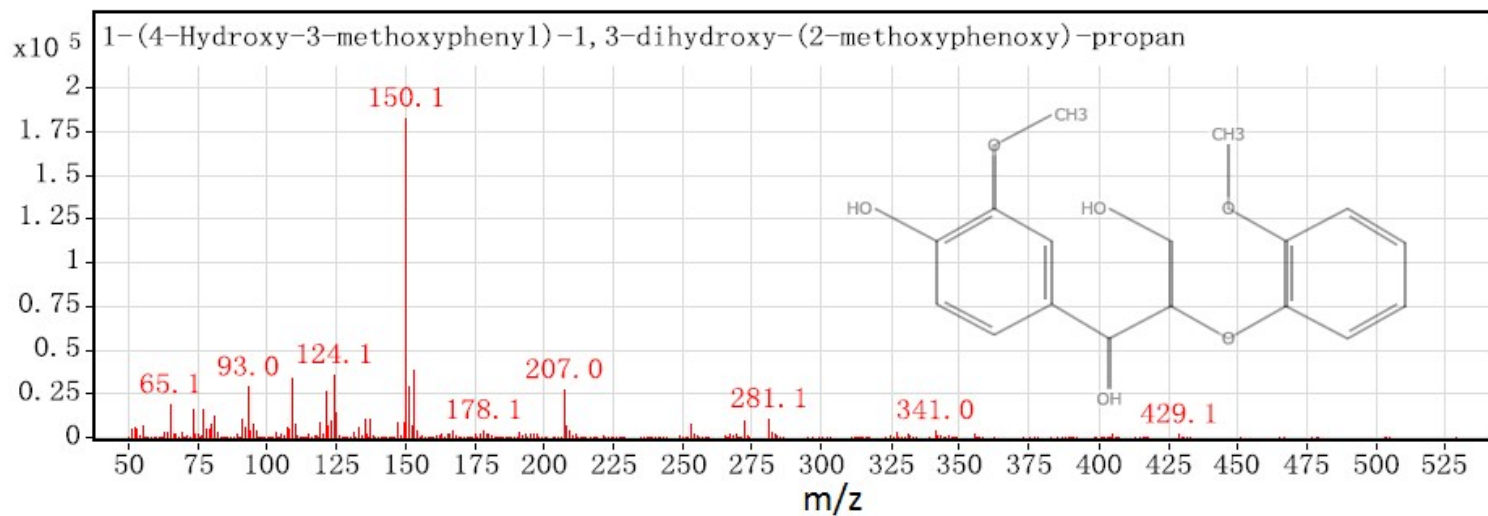


NIST Number	8700
Library	Main library
Total Peaks	22
m/z Top Peak	137
m/z 2nd Highest	196
m/z 3rd Highest	94

Thumbnail

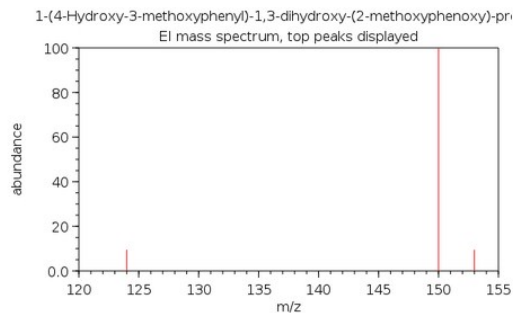


The mass spectrum of 2-Propanone,1-hydroxy-3-(4-hydroxy-3-methoxyphenyl)-**(PHHM)** from GC-MS (Top) and PubChem (Bottom)
Compound CID: 586459
CAS Registry Number: 4899-74-5



NIST Number	312285
Library	Main library
Total Peaks	29
m/z Top Peak	150
m/z 2nd Highest	124
m/z 3rd Highest	153

Thumbnail



The mass spectrum of 1-(4-Hydroxy-3-methoxyphenyl)-1,3-dihydroxy-(2-methoxyphenoxy)-propan (**GG**) from GC-MS (Top) and PubChem (Bottom) Compound CID: 6424189 CAS Registry Number: 7382-59-4

Figure S8. Comparison of mass spectrum between the actually-obtained and the spectroscopy database.

Mass spectrum of C6C3 enol-ether (EE)(Figure S9)

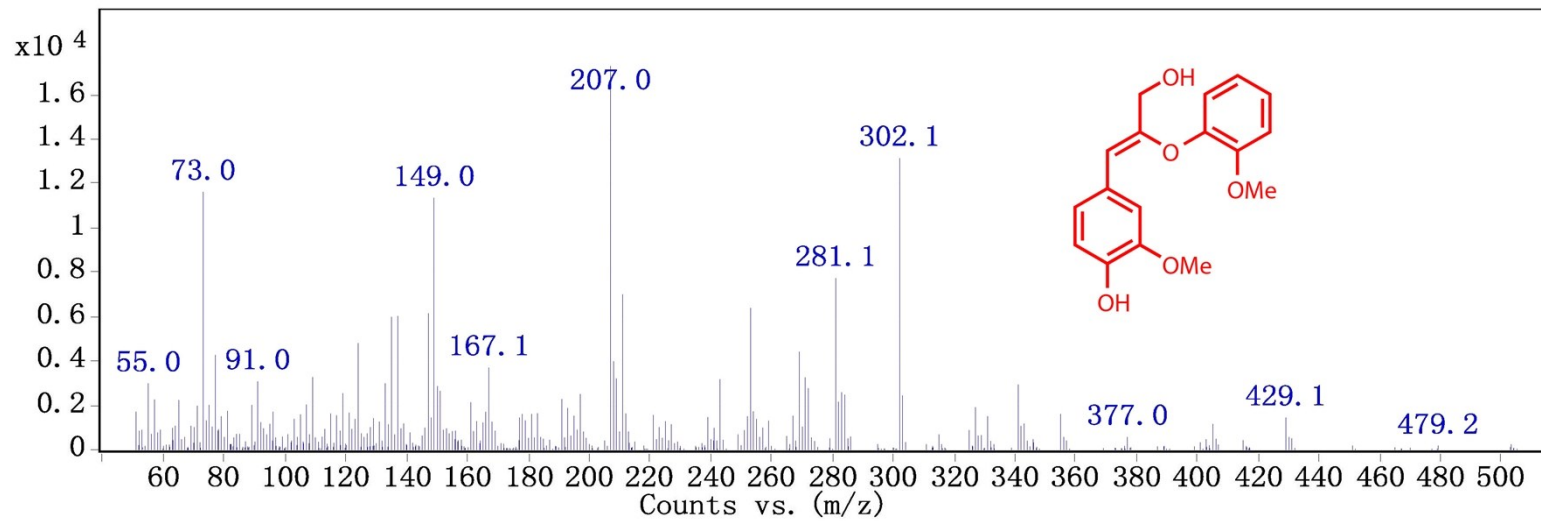


Figure S9. Mass spectrum of C6C3 enol-ether (EE), 3-(4-hydroxy-3-methoxyphenyl)-2-(2-methoxyphenoxy)-2-propenol

Mass spectrum of formylated enol-ether (formylated EE)(Figure S10)

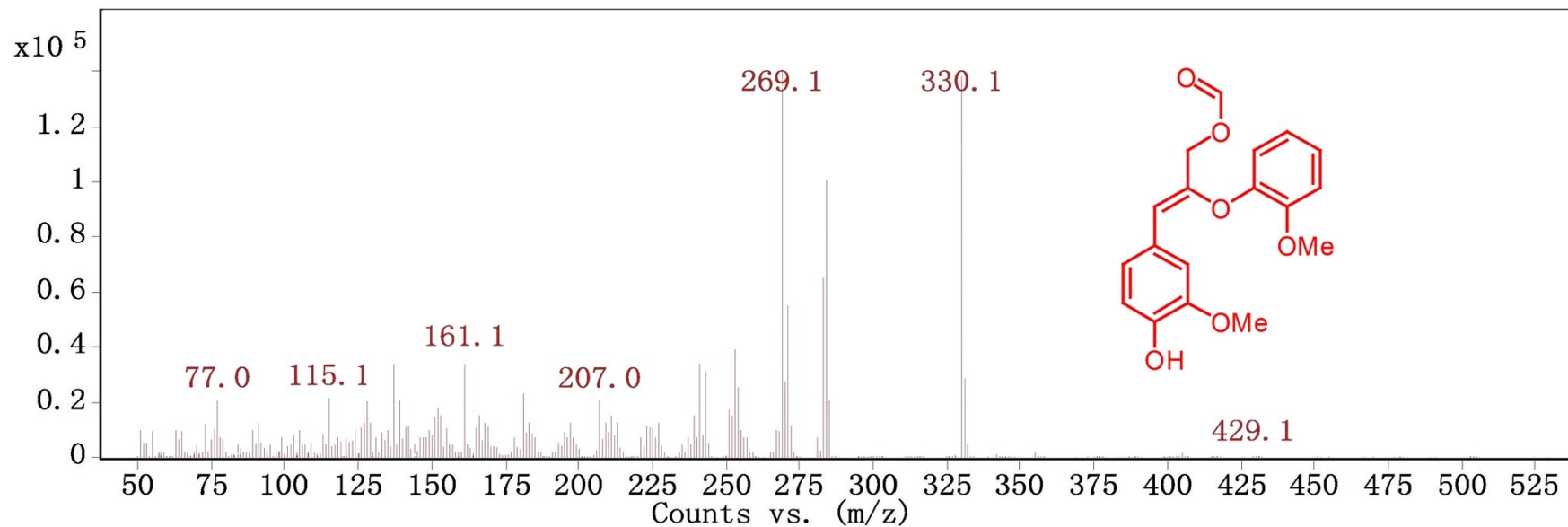


Figure S10. Mass spectrum of formylated enol-ether (EE), 3-(4-hydroxy-3-methoxyphenyl)-2-(2-methoxyphenoxy)-2-propenol methyl ester

Yields of monomeric products from GG degradation(Figure S11)

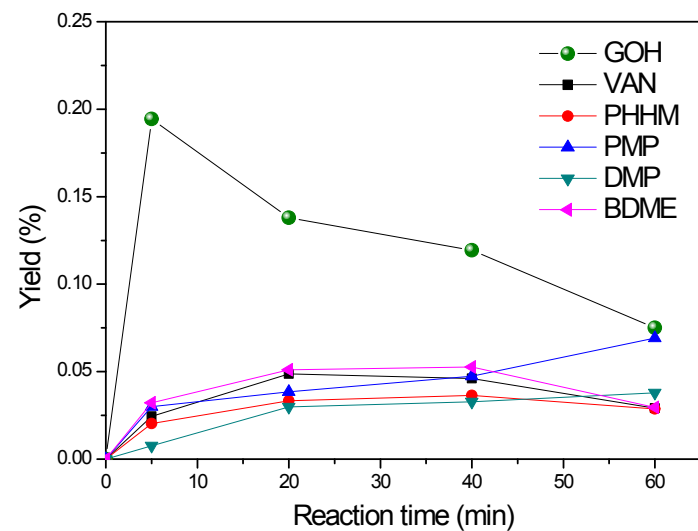


Figure S11. Yields of monomeric products from GG degradation, GOH, VAN, PMP were quantified by GC-MS using standards compounds for calibration, while quantification of PHHM, DMP, and BDME were conducted using calibration curve of VAN.

Assignment of Selected $^{13}\text{C}/^1\text{H}$ Chemical Shifts Observed in HSQC NMR Spectra (Table S1)

Table S1. Assignment of selected $^{13}\text{C}/^1\text{H}$ chemical shifts observed in HSQC NMR Spectra of wheat straw lignin, and quantitative characteristics of MWL of untreated wheat straw, and lignins from RFF fractionation

	$\delta_{\text{C}}/\delta_{\text{H}}$ (ppm)	Assignment	Relative volume integrals							
			F72T120	F72T130	F72T140	F90T120	F90T130	F90T140	MWL	
B_{β}	53.1/3.43	$\text{C}_{\beta}\text{-H}_{\beta}$ in phenylcoumaran substructures (B)	ND ^[a]	ND	ND	ND	ND	ND	ND	0.0019
C_{β}	53.5/3.05	$\text{C}_{\beta}\text{-H}_{\beta}$ in $\beta\text{-}\beta'$ resinol substructures (C)	ND	ND	ND	ND	ND	ND	ND	0.0001
-OCH_3	55.6/3.73	C-H in methoxyls	1	1	1	1	1	1	1	1
A_{γ}	59.4/3.40 and 3.72	$\text{C}_{\gamma}\text{-H}_{\gamma}$ in γ -hydroxylated $\beta\text{-O-}4'$ substructures (A)	0.08	0.085	0.084	0.0832	0.0914	0.0775	0.1428	
I_{γ}	61.3/4.08	$\text{C}_{\gamma}\text{-H}_{\gamma}$ in cinnamyl alcohol end-groups (I)	ND	ND	ND	ND	ND	ND	ND	0.0056
B_{γ}	62.6/3.67	$\text{C}_{\gamma}\text{-H}_{\gamma}$ in phenylcoumaran substructures (B)	0.0546	0.0459	0.0487	0.0658	0.0513	0.0361	0.0321	
A'_{γ}	63.5/3.83 and 4.30	$\text{C}_{\gamma}\text{-H}_{\gamma}$ in γ -acylated $\beta\text{-O-}4'$ substructures (A')	0.0728	0.1054	0.0808	0.1061	0.1044	0.1033	0.0132	
$\text{A}_{\alpha(\text{G})}$	70.9/4.71	$\text{C}_{\alpha}\text{-H}_{\alpha}$ in $\beta\text{-O-}4'$ substructures (A) linked to a G-unit	0.0228	0.0272	0.0234	0.0198	0.0189	0.0089	0.0389	
$\text{A}_{\alpha(\text{S})}$	71.8/4.83	$\text{C}_{\alpha}\text{-H}_{\alpha}$ in $\beta\text{-O-}4'$ substructures (A) linked to a S-unit								
C_{γ}	71.0/3.81 and 4.17	$\text{C}_{\gamma}\text{-H}_{\gamma}$ in $\beta\text{-}\beta'$ resinol substructures (C)	0.0011	0.0013	0.0011	0.0014	0.0011	ND	0.004	
F_{α}	81.2/5.01	$\text{C}_{\alpha}\text{-H}_{\alpha}$ in spirodienone substructures (F)	ND	ND	ND	ND	ND	ND	0.0001	
$\text{A}_{\beta(\text{H})}$	82.9/4.48	$\text{C}_{\beta}\text{-H}_{\beta}$ in $\beta\text{-O-}4'$ substructures (A) linked to a H-unit	0.008	0.0097	0.0081	0.0057	0.0092	ND	0.0053	
$\text{A}_{\beta(\text{G})}$	83.4/4.27	$\text{C}_{\beta}\text{-H}_{\beta}$ in $\beta\text{-O-}4'$ substructures (A) linked to a G-unit	ND	ND	ND	ND	ND	ND	0.0118	
C_{α}	84.8/4.65	$\text{C}_{\alpha}\text{-H}_{\alpha}$ in $\beta\text{-}\beta'$ resinol substructures (C)	0.0001	0.0001	ND	ND	ND	ND	0.0001	
$\text{A}_{\beta(\text{S})}$	85.9/4.10	$\text{C}_{\beta}\text{-H}_{\beta}$ in $\beta\text{-O-}4'$ substructures (A) linked to a S-unit	0.0035	0.0011	0.0009	ND	ND	ND	0.0021	
B_{α}	86.8/5.43	$\text{C}_{\alpha}\text{-H}_{\alpha}$ in phenylcoumaran substructures (B)	0.0018	0.0019	0.0016	0.0015	0.0015	0.0008	0.0033	
T_8	94.1/6.56	$\text{C}_8\text{-H}_8$ in triclin (T)	ND	0.0007	ND	0.0037	ND	ND	0.0218	
T_6	98.7/6.21	$\text{C}_6\text{-H}_6$ in triclin (T)	ND	0.0005	ND	0.0014	0.0005	ND	0.0119	
$\text{S}_{2,6}$	103.8/6.69	$\text{C}_2\text{-H}_2$ and $\text{C}_6\text{-H}_6$ in etherified syringyl units (S)	0.0493	0.066	0.0629	0.0696	0.0655	0.0369	0.0567	
$\text{T}_{2'6'}$	103.9/7.29	$\text{C}_{2'}\text{-H}_{2'}$ and $\text{C}_{6'}\text{-H}_{6'}$ in triclin (T)	0.001	0.0035	0.0008	0.0008	ND	ND	0.0296	

T ₃	104.5/7.02	C ₃ -H ₃ in triclin (T)	ND	0.0013	ND	ND	ND	ND	0.0257
S' _{2,6}	106.3/7.30	C ₂ -H ₂ and C ₆ -H ₆ in α-oxidized syringyl units (S)	ND	0.0002	ND	ND	ND	ND	0.0002
FA ₂	110.6/7.26	C ₂ -H ₂ in ferulate (FA)	0.0011	0.0011	ND	ND	ND	0.0008	0.0012
G ₂	110.9/6.99	C ₂ -H ₂ in guaiacyl units (G)	0.0355	0.0414	0.0388	0.0436	0.0402	0.0225	0.0577
PCA _β and FA _β	113.5/6.27	C _β -H _β in p-coumarate (PCA) and ferulate (FA)	ND	ND	ND	ND	ND	ND	0.0008
G ₅	114.9/6.72 and 6.94	C ₅ -H ₅ in guaiacyl units (G)	0.0884	0.1007	0.0895	0.0910	0.0905	0.0756	0.1037
G ₆	118.7/6.77	C ₆ -H ₆ in guaiacyl units (G)	0.0408	0.0395	0.0281	0.0371	0.0328	0.0185	0.0539
PCA _{3,5}	115.5/6.77	C ₃ -H ₃ and C ₅ -H ₅ in p-coumarate (PCA)	ND	ND	ND	ND	ND	ND	0.0014
H _{2,6}	127.8/7.22	C _{2,6} -H _{2,6} in p-hydroxyphenyl units (H)	ND	ND	ND	ND	ND	ND	0.0029
PCA _{2,6}	130.1/7.45	C ₂ -H ₂ and C ₆ -H ₆ in p-coumarate (PCA)	0.0082	0.0085	0.0072	0.0085	0.008	0.0033	0.0032

[a] Not detected.

Calculation of Various Lignin Moieties by 2D NMR (Table S2)

Table S2. Calculation of various lignin moieties by 2D NMR

Structure	Calculation
C ₉ (total phenylpropane)	$[I(S_{2,6}) + I(S'_{2,6}) + I(S_{\text{condensed}})]/2 + I(G_2) + I(H_{2,6})/2$ *
β-O-4	$[I(A_\alpha) + I(A'_\alpha)] / C_9 \times 100$
β-5	$I(B_\alpha) / C_9 \times 100$
β-β	$I(C_\alpha) / 2 / C_9 \times 100$
Total side ether chains	(β-O-4) + (β-5) + (β-β)
PB	$I(PB_{2,6})/2 / C_9 \times 100$
S	$[I(S_{2,6}) + I(S'_{2,6}) + I(S_{\text{condensed}})]/2 \times 100$
S _{condensed}	$I(S_{\text{condensed}}) / 2 \times 100$
G	$I(G_2) \times 100$
H	$I(H_{2,6})/2 \times 100$

**I* is the integration value of corresponding signal in 2D NMR spectra

Mass balances for RFF treatments of wheat straw and poplar wood (Table S3 and Table S4)

Table S3. Mass balances for RFF treatments of wheat straw under a range of processing conditions

Labels	Conditions ^a			Solid fraction ^b					Dissolved fraction ^b			
	<i>F</i>	<i>T</i>	<i>t</i>	Solid	Glucan	Xylan	Arabinan	Lignin	Glucan	Xylan	Arabinan	Lignin
Wheat straw				100	39.45	22.74	2.57	26.49				
F72T120	72	120	10	63.4	38.9	7.96	0.15	10.12	0.44	14.83	2.25	16.29
F72T130	72	130	10	56.5	39.0	5.79	0.20	8.19	0.49	18.14	2.48	19.12
F72T140	72	140	10	53.2	37.4	4.41	0.04	6.75	0.51	17.00	2.15	20.74
F90T120	90	120	10	53.6	33.4	4.67	0.08	7.66	0.49	14.57	2.34	19.94
F90T130	90	130	10	49.5	30.4	3.10	0.05	6.50	0.61	17.52	2.42	21.34
F90T140	90	140	10	45.3	30.8	2.21	0.04	6.58	0.71	17.61	2.19	21.70

^a *F*, concentration of formic acid (wt%); *T*, treatment temperature (°C); *t*, treatment time (min). ^b All data are yields of components (g) per 100 g (oven-dried weight) untreated wheat straw; the standard deviation of determination is ±2%.

Table S4. Mass balances for RFF treatments of poplar wood under a range of processing conditions

Labels	Conditions ^a			Solid fraction ^b				Dissolved fraction ^b		
	<i>F</i>	<i>T</i>	<i>t</i>	Solid	Glucan	Xylan	Lignin	Glucan	Xylan	Lignin
Poplar wood				100	41.09	17.15	25.12			
F72T120	72	120	30	53.8	38.68	2.98	5.11	0.95	12.21	19.21
F72T130	72	130	30	45.9	39.22	1.58	2.07	1.88	15.01	22.57
F72T140	72	140	30	43.7	37.82	0.99	1.27	2.38	15.67	23.66

^a *F*, concentration of formic acid (wt%); *T*, treatment temperature (°C); *t*, treatment time (min). ^b All data are yields of components (g) per 100 g (oven-dried weight) untreated Poplar wood; the standard deviation of determination is ±2%.

Peaks assignment of 2D $^{13}\text{C}/^1\text{H}$ HSQC NMR of GG degradation products (Table S5)

Table S5. Assignment of 2D $^{13}\text{C}/^1\text{H}$ HSQC NMR chemical shifts of GG, EE, Formylated-EE, PHHM, CD-I, and CD-II

	$\delta_{\text{C}}/\delta_{\text{H}}$ (ppm)	Assignment
-OCH ₃	55.6/3.84	C-H in methoxyls
GG _{α}	70.91/4.75	C _{α} -H _{α} in GG
GG _{β}	83.67/4.27	C _{β} -H _{β} in GG
GG _{γ}	59.83/3.27 and 3.59	C _{γ} -H _{γ} in GG
f-GG _{α}	73.9/6.01	C _{α} -H _{α} in f-GG
f-GG _{β}	80.63/4.56	C _{β} -H _{β} in f-GG
f-GG _{γ}	62.81/3.93 and 4.22	C _{γ} -H _{γ} in f-GG
f _{γ} -EE _{α}	120.6/6.33	C _{α} -H _{α} in f _{γ} -EE
f _{γ} -EE _{γ}	62.81/3.93 and 4.22	C _{γ} -H _{γ} in f _{γ} -EE
formyl at C ₄	161.5/8.29	C-H in formyl at C ₄
formyl at C _{α}	161.8/8.18	C-H in formyl at C _{α}
formyl at C _{γ}	162.5/8.14	C-H in formyl at C _{γ}
PHHM _{α}	44.5/3.67	C _{α} -H _{α} in PHHM
PHHM _{γ}	67.1/4.19	C _{γ} -H _{γ} in PHHM
CD-I _{α}	51.43/4.22	C _{α} -H _{α} in CD-I
CD-I _{β}	81.10/4.89	C _{β} -H _{β} in CD-I
CD-I _{γ}	59.53/3.37	C _{γ} -H _{γ} in CD-I
CD-II _{α}	49.26/4.44	C _{α} -H _{α} in CD-II
CD-II _{β}	91.99/4.54	C _{β} -H _{β} in CD-II
CD-II _{γ}	61.63/3.67	C _{γ} -H _{γ} in CD-II

Literatures

- [1] Z. Wang, S. Qiu, K. C. Hirth, J. Cheng, J. Wen, N. Li, Y. Fang, X. Pan, J. Zhu, *ACS Sustain. Chem. Eng.* **2019**, 7.
- [2] H. Zhou, L. Tan, Y. Fu, H. Zhang, N. Liu, M. Qin, Z. Wang, *Chemsuschem* **2019**, 12, 1213-1221.
- [3] S. Constant, H. L. Wienk, A. E. Frissen, P. de Peinder, R. Boelens, D. S. Van Es, R. J. Grisel, B. M. Weckhuysen, W. J. Huijgen, R. J. Gosselink, *Green Chem.* **2016**, 18, 2651-2665.
- [4] Y. Zhang, Q. Hou, W. Xu, M. Qin, Y. Fu, Z. Wang, S. Willför, C. Xu, *Ind. Crop. Prod.* **2017**, 108, 864-871.